Spectral Sensitization and Supersensitization of AgBr Nanocrystals Studied by Ultrafast Fluorescence Spectroscopy

Igor V. Rubtsov,*,†,§ Kojiro Ebina,† Fuminori Satou,† Ji-Won Oh,† Shigeichi Kumazaki,† Takeshi Suzumoto,‡ Tadaaki Tani,*,‡ and Keitaro Yoshihara*,†

Japan Advanced Institute of Science and Technology, Tatsunokuchi, Ishikawa 923-1292, Japan, Ashigara Research Laboratories, Fuji Photo Film Co., Ltd., Minamiashigara, Kanagawa 250-0193, Japan, and Department of Chemistry, University of Pennsylvania, Philadelphia, Pennsylvania 19104-6323

Received: August 14, 2001; In Final Form: January 5, 2002

Spectral sensitization and supersensitization of the silver bromide nanocrystals were studied by the femtosecond fluorescence up-conversion technique. An annihilation-free fluorescence from J-aggregates of the Dye 1 (3,3′-disulfopropyl-5,5′-dichloro-9-ethylthiacarbocyanine) adsorbed on the silver bromide nanocrystals (edge-to-edge distance from 40 to 900 nm) of different shapes (cubic and octahedral) was measured. Very fast nonexponential fluorescence decays were observed with a fast component from 0.4 to 2.5 ps, and an average decay time from 1.1 to 5.5 ps, depending on the type and size of AgBr grains. The average fluorescence decay time is several times longer on the cubic grains than that on the octahedral grains. Upon addition of a supersensitizer (SS) (3,3′-disulfopropyl-9-ethyl-4,5,4′,5′-dibenzothiacarbocyanine), which is coadsorbed on the surface of silver bromide grains, the fluorescence decay became several times faster with a mean decay time of 0.60−1.3 ps. Different models of supersensitization were examined. The results were analyzed in the framework of the "hole-trapping" supersensitization model. Octahedral grains with different sizes were examined. The effective hole-trapping (electron transfer from SS to the excited J-aggregate) rate constant was found to be independent of the grain size and equal to $\sim$0.60 ps^{-1}. The increase of the electron injection rate (from the excited J-aggregate to the AgBr conduction band) with the increase of the grain size is observed and a possible mechanism is discussed.

1. Introduction

Spectral sensitization is a technology which is used to make the photographic materials sensitive to green and red light by adsorbing sensitizing dyes on the surface of silver halide grains. By photoexcitation of the sensitizing dyes, an electron from the excited state is injected to the conduction band (CB) of the silver halide crystals[1] and used for a latent image formation. A special arrangement of dyes, J-aggregate, is often used to sensitize silver halide grains, since they have a very narrow absorption band (clear color) and can easily be adsorbed on the surface of AgBr grains up to a monolayer coverage.[2]

While the whole scheme of spectral sensitization is known for a long time, the individual processes are not yet well defined. The reason is the experimental difficulties due to high photochemical sensitivity. It was shown in many works that the fluorescence decay of the excited J-aggregates strongly depends on the excitation intensity.[3−5] The origin of this dependence is an exciton−exciton annihilation. The excitation intensity should be kept at a very low level in order to avoid the annihilation. The experiments made at high irradiation intensities are always affected by this process which hides important processes (electron transfer, radiative and nonradiative decays). While several works have been made at sufficiently low excitation intensities, the time resolution was in a range of tens of picoseconds.[6−9] Such a time resolution is not sufficient to observe the initial steps of the photographic sensitization processes. In this work we present the fluorescence study of the excited J-aggregates adsorbed on the AgBr surface with the femtosecond time resolution. The fluorescence decay component as fast as 400 fs is observed.

Generally the structure of J-aggregates adsorbed on the surface is more complicated than that in solution. The static inhomogeneous broadening limits the coherence size[10] and broadens the absorption and fluorescence spectra. Two-dimensional aggregation was reported[11−14] on the AgBr surface, and the hierarchical structure of one-dimensional aggregates was suggested.[15]

Another type of molecule coadsorbed on the AgBr grains in much smaller concentration than the sensitizing dye, which is called supersensitizer (SS), is often used in photography to significantly improve the quantum yield of spectral sensitization, particularly in the red region. Two main mechanisms were proposed for the supersensitization effect. One is the "hole-trapping" mechanism in which the electron from SS fills the hole in the highest occupied molecular orbital (HOMO) of the excited sensitizing dye, since the HUMO level of SS is chosen to be higher than that of the sensitizer.[2,16,17] The resultant ionic state gives up an electron to CB of silver halide with much higher quantum yield. The other is the "aggregate-partitioning" mechanism,[2,18,19] where it is considered that the SS molecules work as J-aggregate partitioners, which decrease the size of the aggregates. This causes an increase in the fluorescence lifetime and/or an increase in the electron injection rate, and hence an increase in the quantum yield of the electron injection.[2,18] (See Section 4.3 for details.) The dynamical studies of the super-

* Authors to whom correspondence should be addressed.
† Japan Advanced Institute of Science and Technology.
‡ Fuji Photo Film Co.
§ University of Pennsylvania.

10.1021/jp013145g CCC: $22.00
Published on Web 03/06/2002

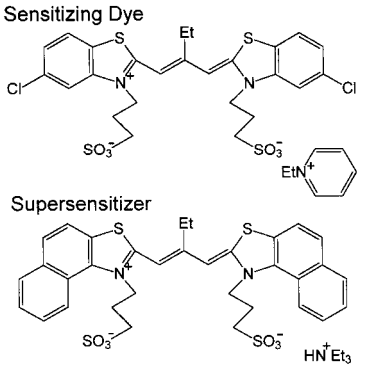

Figure 1. The molecular structure of the sensitizing dye (Dye 1: 3,3′-disulfopropyl-5,5′-dichloro-9-ethylthiacarbocyanine) and the supersensitizer (SS) (Dye 2: 3,3′-disulfopropyl-9-ethyl-4,5,4′,5′-dibenzothiacarbocyanine) used in the present work.

sensitization process are very limited, and restricted to our best knowledge to the case of the "aggregate-partitioning" mechanism.[6,9]

The "hole-trapping" supersensitization mechanism is possible if the HOMO level of the SS is higher than that of J-aggregates, which is true for the Dye 1/Dye 2 (SS) pair studied in this work. In the present work the sensitization and supersensitization processes are studied by the femtosecond fluorescence up-conversion technique to gain knowledge on the "hole-trapping" supersensitization. The time-resolved fluorescence from the sensitizer was observed. The sensitizer used in this work is 3,3′-disulfopropyl-5,5′-dichloro-9-ethylthiacarbocyanine (Dye 1) (Figure 1), which forms J-aggregates on the surface of the AgBr grains. Addition of SS (3,3′-disulfopropyl-9-ethyl-4,5,4′,5′-dibenzothiacarbocyanine) (Figure 1), which is coadsorbed on the AgBr surface, changes the dynamics of the fluorescence decay of the sensitizer. At the same time it changes the quantum yield of the photographic process, which was measured independently. The rate constants of several processes (electron injection, hole-trapping, and the sum of the radiative and nonradiative decays) were determined for the cubic ((100) surface) and octahedral ((111) surface) AgBr nanocrystals. The dependence of the electron injection and the hole-trapping rate constants on the grain size is reported for octahedral nanocrystals.

2. Experimental Section

2.1. Sample Preparation. The emulsions used in this work were composed of the suspension of the AgBr grains in aqueous gelatin solution, and were prepared by the controlled double-jet precipitation method.[20] The edge lengths of the AgBr nanocrystals were 0.2 μm for cubic grains and 0.04,[21] 0.2, 0.4, and 0.9 μm for octahedral grains. The dye molecules were adsorbed on the AgBr grains during the agitation at 40 °C for 20 min of the above-stated emulsions, to which methanol solution of Dye 1 or Dye 1/SS (20/1 molar ratio) was added. The final emulsions contained 88.5 mmol of AgBr and 10.2 g of gelatin and had a pH of 6.6 and pAg of about 7.8. For fluorescence experiments the emulsions were diluted by a 1.5% (g/g) gelatin solution by 10 times, which results in the pAg value of about 6.8. The Dye 1 surface coverage was ~60% of the monolayer.

2.2. Measurements of the Relative Quantum Yield of Spectral Sensitization. The relative quantum yield of spectral sensitization (ψ) is defined as a ratio of a number of photons necessary to create a latent-image center for two types of excitations: at 400 nm excitation into the AgBr conduction band, and the dye excitation by visible light at a wavelength λ.[2,22] It can be expressed by

$$\psi = \frac{N_{400}}{N_\lambda} \tag{1}$$

where N_λ and N_{400} are the numbers of the absorbed photons at λ (in the visible absorption band of the dye) and at 400 nm, respectively, which give the same developed density.[22] It should be noted that both measurements of N_λ and N_{400} should be made with the sample containing the sensitizing dye. The experimental details for the measurements of the relative quantum yield were the same as described in ref 22.

2.3. Time-Resolved Fluorescence Measurements. A femtosecond fluorescence up-conversion setup has been described elsewhere.[23] Briefly, a second harmonic (SH) of the chromium-forsterite femtosecond laser tunable from 610 to 660 nm was used to excite the sample. The pulse duration of the SH pulses was about 44−55 fs at the full width at half-maximum (fwhm), as the spectral width of the pulses was intentionally narrowed to 10−12 nm (fwhm). The repetition rate of the laser is 4 MHz and the diameter of the excited area in the sample was measured to be 0.11 mm, fwhm of the intensity profile of the laser light.

The excitation power, controlled by a neutral density filter before the sample cell, was about 0.1 mW, which corresponds to the excitation intensity of $(0.5-1) \times 10^{12}$ photons/cm^2/pulse. Special care was taken to work at the lowest excitation light intensity so that the effect of the exciton−exciton annihilation process is negligible. No difference in the shapes of the fluorescence decay is observed up to the intensity (flux) of about 6.4×10^{12} photons/cm^2/pulse. At the working level of excitation intensity, $(0.5-3) \times 10^{12}$ photons/cm^2/pulse, the contribution from the exciton−exciton annihilation process is estimated to be less than 2%. The fwhm of the instrument response function was ~98 fs (fwhm), which is much shorter than the characteristic times observed in this work. The excitation wavelength was mostly 620−635 nm (see Table 1). In the measurement on the AgBr grains with 40 nm edge-to-edge length, the laser wavelength was tuned to ~620 nm. The most "red" wavelength was chosen as far as the excitation does not give any contamination of a scattered laser light to the fluorescence signal (Figure 2). The fluorescence signals were detected with a spectral resolution of ±9.5 nm at the central wavelength of about 685 nm (Table 1). During the experiments the sample was circulated by a micropump through a reservoir and an optical path of the sample cell was 0.5 mm. The temperature of the sample during experiments was kept at 50 °C. The photographic quantum yield measurements were made at room temperature. No temperature corrections were made in the analyses of the rate constants, since the temperature effect of the quantum yield is very small.[24] Special care was taken to prevent the sample illumination by the room light during preparation of the sample and the experiment.

3. Results

The time-resolved fluorescence was obtained from the sample that contained AgBr grains with J-aggregates on the surface suspended in gelatin solution. The fluorescence is detected in the red slope of the J-band. The wavelength of observation is tuned according to the fluorescence spectral shift with different types of the AgBr surfaces (Table 1).

The fluorescence decays observed for the 0.2 μm cubic AgBr nanocrystals are shown in Figure 3 for the samples in the presence and absence of SS. The decays are not exponential,

TABLE 1: Results of the Fluorescence Decay Fit with Two Exponentials (τ_1, τ_2, A_1, A_2), Average Time $\bar{\tau}$, and Observed Decay Constant k_{obs} for AgBr Grains of Different Size and Surface Type

AgBr type	AgBr size	λ_{fl}[b] nm	λ_{exc}[c] nm	τ_1 ps	A_1	τ_2 ps	A_2	$\bar{\tau}$ ps	k_{obs} and k_{obs}^{SS} ps^{-1}
cubic (100)	0.2 μm	684	635	1.77	0.64	10.8	0.36	5.0 ± 0.2	0.20 ± 0.01
	0.2 μm+SS	684	635	0.77	0.78	3.35	0.22	1.34 ± 0.06	0.75 ± 0.04
	0.2 μm[a]	680	624	2.5	0.58	9.3	0.42	5.4 ± 0.2	0.19 ± 0.01
	0.2 μm+SS	680	624	0.8	0.87	4.4	0.13	1.3 ± 0.07	0.77 ± 0.05
octahedral(111)	40 nm	680	620	1.5	0.66	13	0.34	5.5 ± 0.7	0.18 ± 0.02
	40 nm+SS	680	620	0.79	0.88	4.5	0.12	1.25 ± 0.15	0.80 ± 0.10
	0.2 μm	684	635	1.08	0.80	5.40	0.20	1.95 ± 0.15	0.51 ± 0.03
	0.2 μm+SS	684	635	0.66	0.84	2.5	0.16	0.95 ± 0.06	1.06 ± 0.06
	0.4 μm	686	634	0.69	0.55	2.26	0.45	1.40 ± 0.07	0.72 ± 0.04
	0.4 μm+SS	686	634	0.56	0.68	1.1	0.32	0.73 ± 0.04	1.37 ± 0.08
	0.9 μm	686	634	0.66	0.85	3.3	0.15	1.07 ± 0.05	0.94 ± 0.04
	0.9 μm+SS	686	634	0.40	0.78	1.35	0.22	0.61 ± 0.03	1.64 ± 0.08

[a] The two experiments are shown for cubic AgBr of 0.2 μm to demonstrate the reproducibility of the measurements, as the grains were newly synthesized for each experiment. [b] The wavelength at which fluorescence dynamics have been measured. [c] The excitation-laser wavelength.

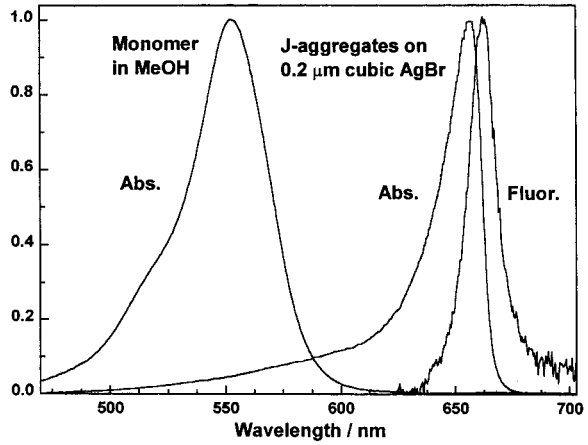

Figure 2. The normalized absorption and fluorescence spectra of Dye 1 J-aggregates on 0.2 μm AgBr. The absorbance was calculated from the measured reflection spectrum using the Kubelka−Munk equation. The steady-state fluorescence spectrum was measured with excitation at 620 nm. The absorbance at the maximum was about 0.1. The absorption spectrum of Dye 1 monomer in methanol is also shown.

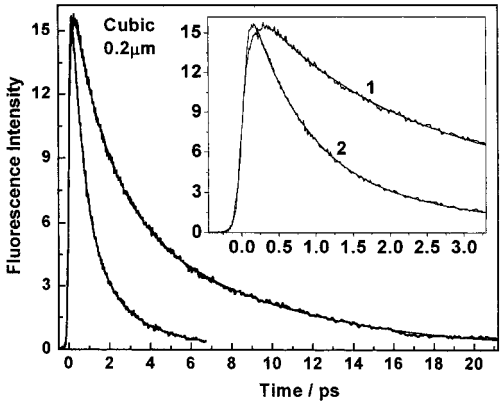

Figure 3. Fluorescence decay signals of Dye 1 on 0.2 μm cubic AgBr grains with (2) and without (1) supersensitizer and two exponential fit. In the inset: the initial parts of the decays are shown. The results of fluorescence-decay curve fitting are given in Table 1.

but a very good fit is obtained by a biexponential decay function. The fluorescence decay of Dye 1 on the 0.2 μm octahedral nanocrystals (without SS) appears to be ~2.5 times faster than that on the cubic nanocrystals (Figures 3 and 4).

Addition of the SS makes the fluorescence decays faster for both cases of the cubic and octahedral nanocrystals (Figures 3 and 4). The effect of SS is significant for the cubic grains, ~4 times, and much smaller for the octahedral grains, 1.6−2.1

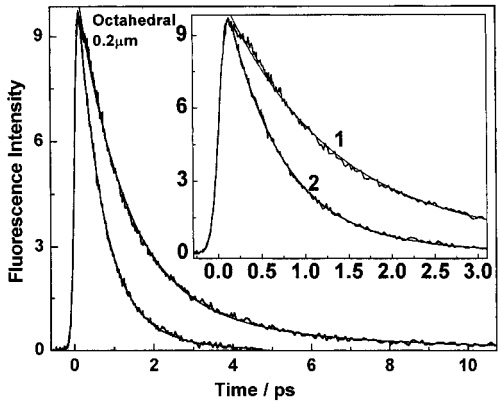

Figure 4. Fluorescence decay signals of Dye 1 on 0.2 μm octahedral AgBr grains with (2) and without (1) supersensitizer. In the inset: the initial parts of the decays are shown. The results of fluorescence-decay curve fitting are given in Table 1.

times, except for the 40 nm grains (see section 4.4). The fluorescence decay signals for all samples studied were fitted by a biexponential decay function ($I(t) = A_1 \exp(-t/\tau_1) + A_2 \exp(-t/\tau_2)$). The results are shown in Table 1. The mean decay times ($\bar{\tau}$) were calculated by eq 2:

$$\bar{\tau} = \frac{A_1\tau_1 + A_2\tau_2}{A_1 + A_2} \qquad (2)$$

The mean observed rate constants $k_{obs} = \bar{\tau}^{-1}$ (Table 1) are used in the analysis instead of individual decay components. The reason for this is a difficulty in separating the two (or more) decay components from each other, as they are not completely independent parameters in the fitting procedure. Generally, it seems that fluorescence decay is more complicated than just a biexponential, and the biexponential fit is used as an approximation sufficient for the noise level of the data we have obtained.

The experiments with various dye-coverage ratios of Dye 1/AgBr on the 40 nm crystals were performed. The fluorescence decays for the relative amount of Dye 1 of 1, 0.1, and 0.025 are shown in Figure 5 (Table 2). At a smaller coverage the size of the J-aggregate is smaller, which is evidenced by a blue shift of the absorption peak of the J-band. When the Dye 1/AgBr ratio is decreased by 10 times, both fast and slow components become slower (Table 2). At the relative dye ratio of 0.025, more than 80% of the dye is in a monomeric form, judging from the absorption spectrum. So, the slow component of curve 3 in Figure 5 mostly reflects the fluorescence decay of the adsorbed monomer in addition to a contribution of small

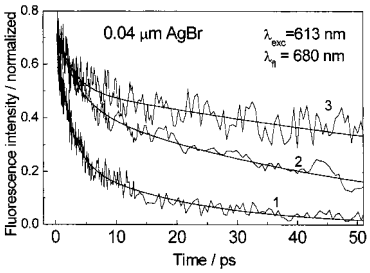

Figure 5. Fluorescence decay signals of Dye 1 on 40 nm AgBr grains with different ratio of Dye 1/AgBr. The amount of AgBr was the same for all experiments and the relative dye concentrations are 1, 0.1, and 0.025 for curves 1, 2, and 3, respectively. The fit parameters for each curve are shown in Table 3. Excitation wavelength for this experiment is 613 nm.

TABLE 2: Two Exponential Fittings for J-Aggregates on 40 nm AgBr Grains with Different Ratio of Dye/AgBr

curve number in Figure 5	relative amount of Dye 1[a]	λ_{max}[b] nm	τ_1 ps	τ_2 ps	A_1	A_2	P,[d] phot./cm^2 $\times 10^{12}$
1	1	640	1.4	12.2	0.60	0.40	1.8
2	0.1	632	3.4	49	0.38	0.62	3.6
3	0.025	630, 572[c]	2.7	120	0.31	0.69	100

[a] The amount of AgBr was same for all experiments. [b] The absorption maximum of J-band. [c] The absorption maximum of monomer. [d] The excitation flux used in each experiment.

aggregates, while the fast component is attributed to J-aggregates. The latter component is affected by the exciton−exciton annihilation process, since the excitation intensity is about 50 times greater for this particular experiment (curve 3), as shown in Table 2.

The slow component of 120 ps of a sample with the smallest dye content is the same as the value obtained by an aggregate "diluting" technique for Dye 1 on 0.17 μm octahedral AgBr grains for 0.5% of the monolayer coverage (120 ps), calculated from Table 2 of ref 9. A similar value has been obtained for Dye 1 on the 0.54 μm octahedral grains with ~6% surface coverage (119 ps),[11] while significantly slower decay (400 ps) has been measured for even smaller surface coverage of 0.6%.[11] However the direct comparison is not possible because different grain sizes were used in these experiments, and also because of the difference in a water content of these samples (dried film in ref 9 and 11 vs emulsion in the present work). It should be noted that in these experiments the excitation wavelength was intentionally shifted to the blue (613 nm), toward monomer absorption, so the contribution from the monomer is larger than that in the other experiments. The important observation is that the fast component of the decay became slower when the Dye 1/AgBr ratio was decreased by 10 times.

Different sizes of AgBr octahedral grains were studied. It was found that the fluorescence decay time decreased with an increase of the grain size from 2 ps for the 0.2 μm grains to 1.1 ps for the 0.9 μm grains (Table 1). This effect is discussed in section 4.4.

4. Discussion

4.1. Characterization of J-aggregates. The coherence size (N), determined as a number of coherently coupled molecules in J-aggregates, can be estimated from the bandwidth of the J-band ($\Delta\nu_{1/2}$(J)) by eq 3,[24] provided that the homogeneous broadening determines the bandwidth.

$$N = (\Delta\nu_{1/2}(\mathrm{M})/\Delta\nu_{1/2}(\mathrm{J}))^2 \quad (3)$$

Here $\Delta\nu_{1/2}$(M) is the bandwidth of the monomer. The spectral bandwidth of the monomer of Dye 1 adsorbed on the AgBr surface was measured at a very low dye concentration when dye is in a form of monomer (more than 90%). The bandwidth obtained, 1250 cm^{-1}, is similar to that in methanol solution, 1324 cm^{-1}.[5] The coherence size calculated by eq 3 is about 7−13. An alternative way to estimate coherence size, N, is based on the spectral shift ($\Delta\nu_N$) of the J-band as a function of N. For linear aggregates it can be determined according to eq 4 as

$$\cos[\pi/(N+1)] = \Delta\nu_N/\Delta\nu_\infty \quad (4)$$

where $\Delta\nu_N$ and $\Delta\nu_\infty$ are the spectral shifts of the aggregates with the coherence size of N and ∞ with respect to the monomer, respectively. Using λ_{max}(M) = 576 nm and λ_{max}(J$_\infty$) = 654 nm for the monomer and the J-aggregates adsorbed on the octahedral grains, the value of N was estimated to be about 10−12. While the spectral width of the J-band, $\Delta\nu_{1/2}$(J), could be affected by inhomogeneous broadening, the spectral shift of the J-band is much less sensitive to that, which makes estimations by eq 4 more reliable. Thus, these estimations show that the coherence size of the J-aggregates of Dye 1 is approximately 10.

4.2. Nonexponentiality of the Fluorescence Decay Dynamics. The fluorescence decay of the J-aggregates on the AgBr surface appears to be very fast and nonexponential. The slowest component that we detected in this work is about 10−15 ps. In the previous works with similar molecular system with a time resolution of tens of picoseconds (the time-correlated single-photon counting method), authors could achieve a higher sensitivity.[5,6] The fast component, however, was not resolved, while several slow components were observed in the range of 20−300 ps.[26] Thus, summarizing both works, we can conclude that fluorescence decay is highly nonexponential with rate components differing by more than 2 orders of magnitude. The origin of the nonexponentiality can generally be discussed in terms of different sites. These sites can be related to different manner of adsorption (different interaction aggregate−surface) as was suggested previously.[5,11] At the same time the aggregate size has some statistical distribution. It is known that the excited-state lifetime in aggregates depends on the size of aggregation due to an increase of the radiative rate constant (superradiance)[27,28] and an increase of the nonradiative rate constant.[9,11,29] The electron injection rate is also dependent on the aggregate size[5,11,19,30] (see section 4.3). The larger the aggregate, the shorter is the lifetime based on the idea of superradiance. The observed nonexponentiality is probably determined by both contributions: the aggregate size distribution and existence of different surface sites. More experiments are needed to specify each contribution. Exciton migration observed in our recent works is also contributing to the nonexponentiality of the fluorescence decay.[31,32]

4.3. Mechanism of Supersensitization. Two mechanisms of supersensitization were previously considered, namely the "aggregate-partitioning"[2,6,18,19] and "hole-trapping"[2,16] mechanisms. In the former mechanism, which is also called as the "exciton-trapping" supersensitization,[16] the J-aggregate size in the presence of a SS is considered to play an essential role.[18] It is assumed that both ends of J-aggregates work as the traps for excitons and as the sites for electron injection. According to this model formation of J-aggregates in the presence of SS makes the J-aggregate size smaller, which gives faster exciton trapping at the sites where the electron-injection rate is supposed to be fast. As a support for the "aggregate-partitioning"

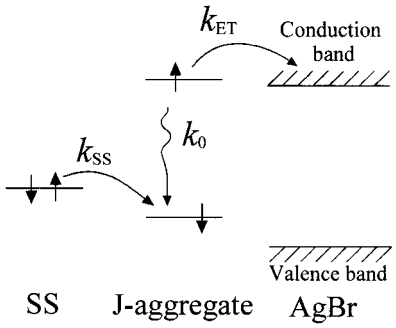

Figure 6. Reaction scheme of the "hole-trapping" supersensitization.

mechanism, the decrease of the injection rate with increase of the J-aggregate size was observed.[5] Contrary to this model an increase of the electron injection rate for larger aggregates has been reported.[30] It should be worth mentioning that all of these experiments observed the slow part of the decay dynamics of the adsorbed dyes.

The "hole-trapping" mechanism of supersensitization was proposed by Gilman.[16] It was suggested that a hole in the HOMO level of excited J-aggregates is filled by electron transfer (ET) from SS followed by electron injection from the reduced J-aggregates to CB of the AgBr grains (Figure 6). To make the hole-trapping process efficient, the HOMO level of SS must be higher than that of J-aggregates. It was reported that the HOMO level of Dye 2 is slightly higher than that of the Dye 1 J-aggregates.[22] So, we propose that for the present system of Dye 1/Dye 2 (SS) the "hole-trapping" mechanism can be the main mechanism of supersensitization. The following observations support this statement.

The increase in the sum of the trapping and injection rates by about 5 times was observed upon addition of SS. In the presence of SS the J-band becomes slightly broader, which can be assigned to a smaller size of the aggregates, as well as to a change of the environment for J-aggregates in the presence of SS. Even if one attributes the absorption peak broadening upon addition of SS solely to a shortening of the aggregates, the change of the coherence size would be small, for example, decreasing from 10 to 6 in the absence and presence of SS, respectively. We think it is unrealistic to attribute such a large change of the rates to a slight change of the coherence size. As an alternative possibility of energy transfer from J-aggregate to SS and electron transfer from SS to AgBr could be considered. However, we think this model is not applicable to the present system. Addition of SS causes a slight red shift and broadening and so-called mixed aggregates are formed.[33] In the excited state of the mixed J-aggregate there seems to be no single separable state for SS and the excitation is delocalized in the whole region. The efficiency of supersensitization in the typical "hole trapping" mechanism[16] is dependent on the oxidation potential of SS and not on the sensitization efficiency of SS itself. All of these observations drove us to apply the hole trapping mechanism.

The experiments with different amount of Dye 1 adsorbed on the surface of AgBr grains further support this assumption (Figure 5 and Table 2). At smaller ratio of Dye/AgBr the average size of J-aggregates is smaller. Upon decreasing of the ratio of Dye/AgBr by 10 times, the fast component of the decay became slower (Figure 5 and Table 2). This is not in favor for the "aggregate-partitioning" (or "exciton trapping") mechanism in the present system. Thus, we consider that this mechanism is not the major mechanism and its contribution is negligible in the present systems.

In the framework of the "hole-trapping" model the scheme shown in Figure 6 is proposed. Here k_{ET} is the rate constant of the electron injection from the excited dye to AgBr, k_{SS} is the rate constant of ET from SS to the excited dye, and k_0 is the total (radiative and nonradiative) decay rate constant of the excited J-aggregates. The observed ET rate in the absence and presence of SS is expressed as

$$k_{obs} = k_{ET} + k_0 \tag{5}$$

$$k_{obs}^{SS} = k_{ET} + k_0 + k_{SS} \tag{6}$$

In the analysis the observed rate constants k_{obs} and k_{obs}^{SS} are calculated from the average fluorescence lifetimes $k_{obs} = \bar{\tau}^{-1}$ (see eq 2). In the present model both k_{ET} and k_0 are assumed be independent of the presence of SS, even though SS may decrease slightly the aggregate coherence size. The value of k_{SS} can be calculated by a difference: $k_{obs}^{SS} - k_{obs}$. The results are shown in Table 3. It is worth mentioning that the values of k_{SS} are similar for all cases (Table 3) with an average value of about 0.60 ps^{-1}.

The relative quantum efficiency of the photographic process was determined by the independent experiments (see Experimental Section). The results are shown in Table 3 as ψ and ψ_{SS}, obtained in the absence and presence of SS, respectively. Using these values and the fluorescence decay data, one can estimate the values of k_{ET} and k_0 and the quantum efficiency of the photoinduced electron injection. For that let us derive equations for the quantum yield of the AgBr photoreduction.

The quantum yield of the electron injection from J-aggregates to AgBr, when no SS is added, is expressed as

$$\varphi = \frac{k_{ET}}{k_{obs}} \tag{7}$$

In this case the electron injection rate is competing with the radiative and nonradiative decay rate k_0. Addition of SS induces an additional reaction, i.e., electron transfer from SS to the excited J-aggregate (k_{SS}). The products of this reaction are the reduced J-aggregate and the cation of SS. Let us introduce the quantum yield of electron injection from the reduced J-aggregate to the CB of AgBr as φ_-. The total quantum yield of the AgBr photoreduction in the presence of SS can be expressed as

TABLE 3: Results of the Data Analysis in the Framework of the "Hole-Trapping" Model

AgBr size & type[a]	λ_{max} nm	ψ	ψ_{SS}	k_{obs} ps^{-1}	k_{obs}^{SS} ps^{-1}	k_{SS} ps^{-1}	η	k_{ET} ps^{-1}	k_0 ps^{-1}	φ	φ_{SS}	k'_{ET} ps^{-1}
0.2 Cub	657	0.38	0.92	0.20	0.75	0.55 ± 0.05	1.09	0.070 ± 0.012	0.13	0.35	0.84	
0.2 Cub	658	0.36	0.84	0.19	0.77	0.58 ± 0.05	0.99	0.067 ± 0.012	0.12	0.36	0.85	
0.04	640			0.18	0.8	0.62 ± 0.12						<0.1
0.2 Oct	652	0.6	0.72	0.51	1.06	0.55 ± 0.10	0.83	0.37 ± 0.07[b]	0.15	0.72	0.87	0.33
0.4 Oct	652	0.67	0.82	0.72	1.36	0.65 ± 0.14	0.98	0.49 ± 0.08	0.23	0.68	0.83	0.54
0.9 Oct	651	0.61	0.65	0.94	1.64	0.70 ± 0.12	0.72	0.80 ± 0.15[b]	0.15[b]	0.85	0.90	0.76

[a] In μm. [b] Averaging of several data sets for independently prepared emulsions results in the k_{ET}(0.2 Oct) = 0.39 ps^{-1}, and k_{ET}(0.9 Oct) = 0.82 ps^{-1}, k_0(0.9 Oct) = 0.17 ps^{-1}.

$$\varphi_{SS} = \frac{k_{ET}}{k_{obs}^{SS}} + \frac{k_{SS}}{k_{obs}^{SS}}\varphi_{-} \tag{8}$$

where the first term stands for the electron injection from the excited J-aggregates, and the second term consists of the quantum yield of the reduced J-aggregate formation multiplied by the quantum yield of the AgBr reduction by the reduced J-aggregate (φ_{-}).

Finally, it was pointed out recently[22] that the relative quantum yield of spectral sensitization (ψ and ψ_{SS}) are not always equal to the quantum yield of the electron injection from the dye to silver halide grains (φ and φ_{SS}). The reasons, which are related to the structure and size of AgBr grains, are discussed by Suzumoto and Tani.[22] Then the relative quantum yield can be expressed as

$$\psi = \varphi\eta = \frac{k_{ET}}{k_{obs}}\eta \tag{9}$$

where η is the deviation factor between ψ and φ. We use the same η value for the experiments in the presence and absence of SS for the same size of the AgBr grains produced under the same conditions. The relative quantum yield for spectral sensitization in the presence of SS (ψ_{SS}) can be expressed as

$$\psi_{SS} = \varphi_{SS}\eta = \left(\frac{k_{ET}}{k_{obs}^{SS}} + \frac{k_{SS}}{k_{obs}^{SS}}\varphi_{-}\right)\eta \tag{10}$$

Then from eqs 9 and 10, η can be derived as

$$\eta = \frac{\psi_{SS}k_{obs}^{SS} - \psi k_{obs}}{k_{SS}\varphi_{-}} \tag{11}$$

Using eq 11 the $\eta\varphi_{-}$ values were calculated. For the 0.2 μm cubic AgBr grains, where η value is reported to be equal to 1 and the value $\eta\varphi_{-}$ is about 1. This means that the electron injection rate from the reduced J-aggregate to the AgBr conduction band is much higher than the electron-transfer rate to oxidized SS. This is supported by the observation that the energy level of the electron in the reduced J-aggregate is higher than that of the excited J-aggregate, which should increase the injection rate.[17] At the same time, the back electron-transfer reaction from the reduced J-aggregate to the oxidized SS is expected to be in the Marcus-inverted region. On this basis, we use $\varphi_{-} = 1$ for all grain types. The rate constants k_{ET} and k_0 were calculated according to eqs 12 and 13 as

$$k_{ET} = \frac{\psi k_{obs}}{\eta} \tag{12}$$

$$k_0 = k_{obs} - k_{ET} \tag{13}$$

The calculated η, k_{ET}, and k_0 values for different sizes and surfaces of the AgBr grains are shown in Table 3. The values of k_0 are similar for cubic and octahedral grains. There is no clear dependence of k_0 upon grain size for octahedral grains. The electron injection rate, k_{ET}, is about 5.5 times smaller for cubic grains compared with the octahedral grains of the same size. The increase of k_{ET} with the grain size is observed for the octahedral grains (Figure 7), which will be discussed in the next section. The rate constant of electron transfer from SS to the excited J-aggregates, k_{SS}, is larger than k_{ET} by about 8 times for cubic and only about 1.5 times for octahedral grains. This determines the relatively high quantum yield of the photographic process with octahedral grains and the rather small improvement by addition of SS. On the cubic grains the quantum yield without SS is small due to the small value of the k_{ET} rate constant. Therefore a large increase of the quantum yield in the presence of SS is observed due to a large value of the k_{SS} constant in comparison with k_{ET}, namely $k_{SS} \sim 8k_{ET}$ for cubic grains.

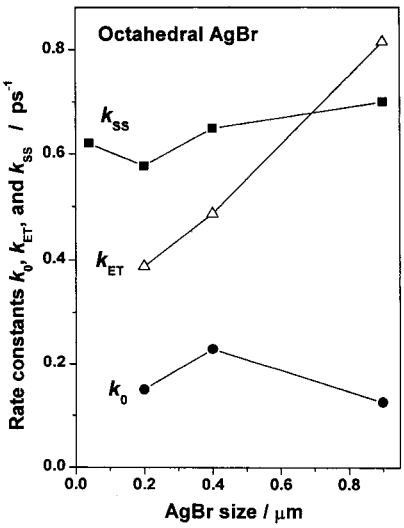

Figure 7. The calculated rate constants (k_0, k_{ET}, and k_{SS}) as a function of AgBr grain size for octahedral grains. Here k_{ET} is the electron-injection rate constant from the excited dye to AgBr, k_{SS} is the electron-transfer rate constant from supersensitizer to the excited dye, k_0 is the total (radiative and nonradiative) decay rate constant of the excited J-aggregates.

4.4. Grain-Size Dependence. We observed that the fluorescence decay rate k_{obs} depends on the grain size for the octahedral grains (Table 1). The size dependencies of the k_{ET}, k_{SS}, and k_0 rate constants are shown in Figure 7 and Table 3. While k_{SS} and k_0 are not much dependent on the grain size, k_{ET} increases about twice with the increase of the grain size from 0.2 to 0.9 μm. Since k_0 does not depend on the grain size, the average value ($\overline{k_0}$) was calculated to be 0.18 ps^{-1}. Using this value the electron injection rate (denoted in the Table 3 as k_{ET}') can be calculated by using only experiments with Dye 1 without SS (k_{obs}), and $\overline{k_0}$ (eq 5). The advantage of this procedure is that the data of the relative quantum yield, which contain some scatter, are not used, while $\overline{k_0}$ is taken as known and constant. The values of k_{ET}' are very close to that obtained by eq 12 (k_{ET}) (Table 3). This confirms that the above conclusions are stable to some variations of the parameters.

It should be mentioned that the fluorescence decay and particularly the electron injection rate depends on the aggregate size.[5,11,31] Therefore, in this experiment the size of aggregates on different grains (coherent length) was controlled to be the same, judging from the position and width of the absorption spectrum of J-aggregates.

Next, let us consider the origin of the size dependence of k_{ET}. It is well-known that the potential energy surface is bent near the surface of the semiconductor crystals, as formalized by the charge space theory.[34,35] The charged layer in AgBr grains is formed by the excess of the positive interstitial defects (Ag^+) near the surface. As a result, a double layer is formed with the positively charged interior and negatively charged surface of the grains.[36] The excess positive charge is distributed near the surface of the grains with a rapid decrease of its concentration toward the interior. The characteristic distance of the potential drop, which is called the Debye length, for the case of thick pure crystal, is about 0.14 μm.[35,37] The potential difference

between the (111) surface and the interior for thick AgBr crystals was measured to be about 0.22 eV.[38] If the grain size is comparable or smaller than the Debye length for thick crystals, the potential level inside grains becomes dependent on the grain size. For example, the estimated potential in the middle of the grain relative to the surface potential is 205 mV for 0.9 μm grains, 165 mV for 0.4 μm grains, and 110 mV for 0.2 μm grains.[39] The described space-charge layer exists even in an isolated grain in a vacuum. In this case the potential at the surface is considered to remain constant for the grains of different sizes,[40] as it depends only on the difference in the free energies of formation of interstitials and vacancies at the surface.[41] In solution the picture is more complicated. There is an additional double layer between the surface and solution, which depends on pAg of solution.[40,42] The pAg in the experiment was about 6.8, which is higher than pAg corresponding to the point of zero charge (pzc) of 5.4.[43] In this case, the grains will be charged negatively with the counter layer in solution, which contains excess cations.

The sensitizing dye (J-aggregate) is adsorbed on the surface and injects an electron into the conduction band. As the distance of the effective electron injection ($<$1 nm) is much smaller than the Debye length ($\sim$0.14 μm) the surface potential (not potential of the grain interior) is effective for the electron injection process. While for isolated grains the surface potential is considered to be constant, the situation in the solution is not so clear. We suggest that the surface potential is slightly different for the grains of different sizes due to the influence of the two double layers. The experiment shows that k_{ET} increases about twice when going from 0.2 to 0.9 μm grains. This difference corresponds to the difference in the barrier for electron injection of about 17 mV, which gives about 30 mV difference in the values of surface potential energy.[44] The calculated difference between the interior and surface potentials is about 205 mV for the 0.9 μm grains, and 115 mV for 0.2 μm grains. Thus, the expected shift of the surface potential is much smaller than the differences in the internal potential, which makes the present explanation possible.

It is difficult to compare the injection rate observed for 40 nm grains with that of the larger octahedral grains. The main reason is that the size of the aggregates adsorbed on the 40 nm grains is much smaller than that on the larger grains, judging from the position and width of the J-peak (Table 3). So the slow fluorescence decay rate observed in 40 nm crystals is probably caused by the smaller aggregate size.

Our data can be compared with the results obtained previously by the time-correlated single-photon counting technique.[5,6,9] The fluorescence decay times obtained for the J-aggregates of Dye 1 adsorbed on the AgBr octahedral grains ranges from 7 ps (on 0.8 μm grains)[5] to $\sim$25 ps (on 0.17 and 0.8 μm grains),[6,9] which all are much larger than that obtained in the present work ($\sim$2 ps for 0.2 μm and $\sim$1.1 ps for 0.9 μm octahedral grains). As a result, the k_{ET} values obtained in this work are much greater than those previously reported; for example, k_{ET} of 0.51 ps^{-1}, obtained here for 0.2 μm octahedral grains, is more than 1 order of magnitude greater than that ($\sim$0.03 ps^{-1}) calculated from ref 9. The origin of the discrepancies can be 2-fold. First, the time resolution used in the previous works[5,6,9] was limited by the instrument response function (IRF) by 2 orders of magnitudes (about 30$-$70 ps). At the same time, the fluorescence decay signals are strongly nonexponential, which does not allow one to get proper decay times by deconvolution procedure for the decay times shorter than the width of IRF. Second, the dried films were studied in previous works, which may affect the electron injection rate, for example through the difference in the pAg values.[31]

Conclusions

The primary processes of the photographic sensitization were studied with a sub-hundred-femtosecond time resolution. The time-resolved fluorescence measurements in combination with the photographic quantum yield measurements were applied to molecular systems with sensitizer and supersensitizer (SS) adsorbed in form of J-aggregates on the surface of AgBr grains. Two types of AgBr nanocrystals, cubic and octahedral, were examined. The electron injection rate on the cubic grains is found to be about 8 times slower than that on the octahedra. The lifetime of the excited state of J-aggregates depends significantly on the presence of the supersensitizer. The hole-trapping rate (electron transfer from SS to the excited J-aggregate) is found to be similar for the cubic and octahedral grains of 0.2 μm size. The k_0 (the sum of the radiative and nonradiative rate constants) was found to be independent of the grain size for octahedral grains. The electron injection rate (k_{ET}) was found to increase about twice with the increase of the grain size of the octahedral grains from 0.2 to 0.9 μm. A shift of the surface potential is suggested as a reason of the grain-size dependence of the injection rate.

Acknowledgment. This work is supported in part by the grant-in-aid program for scientific research (12640554) of the Ministry of Education, Science, Sports, and Culture of Japan.

References and Notes

(1) Gurney, R. W.; Mott, N. F. *Proc. R. Soc.* **1938**, *A164*, 151.
(2) Tani, T. *Photographic Sensitivity*; Oxford University Press: Oxford, 1995; p 142.
(3) Brumbaugh, D. V.; Muenter, A. A.; Knox, W.; Mourou, G.; Wittmershaus, B. *J. Lumin.* **1984**, *31*$-$*32*, 783.
(4) Sundström, V.; Gillbro, T.; Gadonas, R. A.; Piskarskas, A. *J. Chem. Phys.* **1988**, *89*, 2754.
(5) Kemnitz, K.; Yoshihara, K.; Tani, T. *J. Phys. Chem.* **1990**, *94*, 3099.
(6) Tani, T.; Suzumoto, T.; Kemnitz, K.; Yoshihara, K. *J. Phys. Chem.* **1992**, *96*, 2778.
(7) Trosken, B.; Willig, F.; Schwarzburg, A.; Ehret, A.; Spitler, M. *J. Phys. Chem.* **1995**, *99*, 5152.
(8) Scheblykin, I. G.; Varnavsky, O. P.; Bataiev, M. M.; Sliusarenko, O.; De.; Van der Auweraer, M.; Vitukhnovsky, A. G. *Chem. Phys. Lett.* **1998**, *298*, 341.
(9) Muenter, A. A.; Brumbaugh, D. V.; Strati, G.; Hailstone, R. K. In *International Congress on Imaging Science*; University of Antwerp: Belgium, 1998; p 166.
(10) Durrant, J. R.; Knoester, J.; Wiersma, D. A. *Chem. Phys. Lett.* **1994**, *222*, 450.
(11) Lanzafame, J. M.; Muenter, A. A.; Brumbaugh, D. V. *Chem. Phys.* **1996**, *210*, 79.
(12) Asanuma, H.; Tani, T. *J. Phys. Chem. B* **1997**, *101*, 2149.
(13) Kawasaki, M.; Inokuma, H. *J. Phys. Chem. B* **1999**, *103*, 1233.
(14) Furuki, M.; Wada, O.; Pu, L. S.; Sato, Y.; Kawashima, H.; Tani, T. *J. Phys. Chem. B* **1999**, *103*, 7607.
(15) Kobayashi, T.; Misawa, K. *J. Lumin.* **1997**, *72*$-$*74*, 38.
(16) Gilman, P. B. *Photogr. Sci. Eng.* **1974**, *18*, 418.
(17) Tani, T.; Suzumoto, T.; Ohzeki, K. *J. Phys. Chem.* **1990**, *94*, 1298.
(18) Rosenoff, A. E.; Norland, K. S.; Ames, A. E.; Walworth, V. K.; Bird, G. R. *Photogr. Sci. Eng.* **1968**, *12*, 185.
(19) West, W.; Carrol, B. H. *J. Chem. Phys.* **1947**, *15*, 529; *J. Chem. Phys.* **1951**, *19*, 417.
(20) Berry, C. R.; Skillman, D. C. *Photogr. Sci. Eng.* **1962**, *6*, 159.
(21) The small grains of 40 nm were prepared by the same method as octahedral grains, although the shape is nearly spherical and surfaces other than (111) may appear in these grains.
(22) Suzumoto, T.; Tani, T. *J. Im. Sci. Technol.* **1996**, *40*, 56.
(23) Rubtsov, I. V.; Shirota, H.; Yoshihara, K. *J. Phys. Chem. A* **1999**, *103*, 1801.
(24) Tani, T. *Photogr. Sci. Eng.* **1984**, *28*, 150.
(25) Knapp, E. W. *Chem. Phys.* **1984**, *85*, 73.
(26) The experiments of ref 5 were made with a dry film, while in this work the sample is a water/gelatin emulsion. The presence of a larger amount

of water may change slightly the characteristic decay times, but cannot change general features. Thus, no large difference is expected between these two sample conditions.

(27) Fidder, H.; Terpstra, J.; Wiersma, D. A. *J. Chem. Phys.* **1991**, *94*, 6895.

(28) Spano, F. C.; Kuklinski, J. R.; Mukamel, S. *J. Chem. Phys.* **1991**, *94*, 7534.

(29) Sundström, V.; Gillbro, T. A. *J. Chem. Phys.* **1985**, *83*, 2733.

(30) Muenter, A. A.; Brumbaugh, D. V.; Apolito, J.; Horn, L. A.; Spano, F. C.; Mukamel, S. *J. Phys. Chem.* **1992**, *96*, 2783.

(31) Rubtsov, I. V.; Ebina, K.; Yoshihara, K.; Knoester, J.; Suzumoto, T.; Tani, T. *Ultrafast Phenomena XII*;Elsaesser, T., Mukamel, S., Murnane, M. M., Scherer, N. F., Eds.; Springer-Verlag: Berlin, 2000; p 444.

(32) Oh, J.-W.; Kumazaki, S.; Rubtsov, I. V.; Suzumoto, T.; Tani, T.; Yoshihara, K. *Chem. Phys. Lett*., in press.

(33) The J-aggregate of SS by itself, without coadsorption with Dye 1, is observed to be located at 684 nm. In the present system of coadsorption we do not observe any band at this position.

(34) Frenkel, J. *Kinetic Theory of Liquids*; Oxford University Press: New York, 1946.

(35) Tan, Y. T.; Hoyen, H. A., Jr. *Surf. Sci.* **1973**, *36*, 242.

(36) Saunders, V. I.; Tyler, R. W.; West, W. *Photogr. Sci. Eng*. **1968**, *12*, 90.

(37) Trautweller, F. *Photogr. Sci. Eng*. **1968**, *12*, 98.

(38) $\varphi_S = 0.22$ eV (Oct). Unpublished results from T. Tani.

(39) The values were estimated by scaling of the potential energies calculated in ref 34. The scaling factor was 0.22/0.14 which corresponds to the ratio of measured and calculated bending potential energies.

(40) Hoyen, H. A., Jr. *Photogr. Sci. Eng*. **1973**, *17*, 188.

(41) This is valid in approximation of large number of surface states (see ref 40 for details).

(42) Kruyt, H. R. *Colloid Science*, Vol. 1; Elsevier: Amsterdam, 1983.

(43) Honig, E. P.; Hengst, J. H. Th. *J. Colloid Interface Sci.* **1969**, *31*, 545.

(44) The classical Marcus−Levich−Jortner theory was used to estimate the energy difference between the excited state of dye and the conduction band of AgBr. The level of the excited dye was considered to be close to the conduction band. The result is weakly dependent on the reorganization energy in the range of reported values, from 50 meV[6] to 200 meV.[9]